OXFORD

Social Cognitive and Affective Neuroscience, 2017, 861–870

doi: 10.1093/scan/nsx015
Advance Access Publication Date: 17 February 2017
Original article

Sensitivity to perception level differentiates two subnetworks within the mirror neuron system

Shiri Simon and Roy Mukamel

Sagol School of Neuroscience and School of Psychological Sciences, Tel-Aviv University, Tel Aviv 69978, Israel

Correspondence should be addressed to Roy Mukamel, Sagol School of Neuroscience and School of Psychological Sciences, Tel-Aviv University, Tel Aviv 69978, Israel. E-mail: rmukamel@post.tau.ac.il

Abstract

Mirror neurons are a subset of brain cells that discharge during action execution and passive observation of similar actions. An open question concerns the functional role of their ability to match observed and executed actions. Since understanding of goals requires conscious perception of actions, we expect that mirror neurons potentially involved in action goal coding, will be modulated by changes in action perception level. Here, we manipulated perception level of action videos depicting short hand movements and measured the corresponding fMRI BOLD responses in mirror regions. Our results show that activity levels within a network of regions, including the sensorimotor cortex, primary motor cortex, dorsal premotor cortex and posterior superior temporal sulcus, are sensitive to changes in action perception level, whereas activity levels in the inferior frontal gyrus, ventral premotor cortex, supplementary motor area and superior parietal lobule are invariant to such changes. In addition, this parcellation to two sub-networks manifest as smaller functional distances within each group of regions during task and resting state. Our results point to functional differences between regions within the mirror neurons system which may have implications with respect to their possible role in action understanding.

Key words: fMRI; mirror neuron system; conscious perception; action observation

Introduction

Mirror neurons are a specialized subset of brain cells with visuo-motor properties that discharge during both action execution and passive observation of actions performed by others. These cells were originally discovered in the ventral premotor cortex of the macaque monkey (area F5) (Dipellegrino *et al.*, 1992; Gallese *et al.*, 1996; Rizzolatti *et al.*, 1996) and were subsequently demonstrated in other areas in the human and non-human motor pathway (Gallese *et al.*, 2002; Fogassi *et al.*, 2005; Gazzola and Keysers, 2009; Caspers *et al.*, 2010; Mukamel *et al.*, 2010; Molenberghs *et al.*, 2012). These areas—largely consisting of the primary and premotor cortices, the inferior frontal gyrus and parietal regions—were termed the mirror neuron system (MNS).

While the existence and anatomical distribution of cells with mirroring properties is now widely accepted, there is still strong debate with respect to the functional significance and the source from which such cells gained their capacity to match observed with executed actions (Heyes, 2010; Hickok, 2009, 2013). One account suggests that mirroring properties have a role in cognitive functions such as action and intention understanding. In support of this view are physiological evidence in primates which indicate that mirror neuron responses are sensitive to action goals rather than specific low-level kinematics (Rizzolatti and Sinigaglia, 2010; Rizzolatti and Fogassi, 2014). For example, observation of actions with similar kinematics but different action goals have been shown to evoke different neural responses in fronto-parietal mirror neurons (Umilta *et al.*, 2001; Fogassi *et al.*, 2005; Iacoboni *et al.*, 2005). A complementary evidence demonstrates that different action kinematics having the same goal evoke similar neural response (Umilta *et al.*, 2008). Additionally, recent neuropsychological studies on patients with temporal, parietal, and frontal lesions are consistently

Received: 12 September 2016; **Revised:** 17 December 2016; **Accepted:** 29 January 2017

associated with poor performance in tasks of action perception and understanding (Urgesi *et al.*, 2014). Nonetheless, an alternative account suggests that the MNS does not represent action and intention understanding and that the functional properties of mirror neurons are merely a byproduct of associative learning formed through sensorimotor experience which is gained during the course of individual development (Del Giudice *et al.*, 2009; Hickok, 2009; Heyes, 2010). This is supported by the fact that the activity within the mirror system can be dynamically remapped with training (Catmur *et al.*, 2007; Press *et al.*, 2007; Catmur *et al.*, 2011). According to Csibra, understanding the actions and intentions of others is achieved outside the motor system, and action mirroring is the consequence of later processing (Csibra, 2007).

It is plausible that mirror neurons which are distributed over distinct regions within the sensorimotor system, hold diverse functional roles. While mirror neurons in some regions might have a role in coding the goal of an action, in other regions such functional properties may have evolved as a result of extensive simultaneous experience in which specific observed and executed actions are temporally correlated. Since understanding of goals requires conscious perception of the relevant action, we should expect that mirror neurons potentially involved in action goal coding, will be modulated by changes in the level of action perception. A recent behavioral study demonstrated that masked implied-action primes affected motor preparation and execution only when they were consciously perceived. Nonetheless, subsequent action perception was affected by the primes, also when they were not consciously perceived (Mele *et al.*, 2014). We have recently shown, that EEG mu and beta oscillation power over sensorimotor cortices are modulated by the level of action perception (Simon and Mukamel, 2016). Oscillation power over sensorimotor regions in these frequency bands serve as index to infer mirror neuron activity (Pineda, 2005). While in our EEG study consciously perceived actions were associated with stronger mu and beta suppression, the EEG response was also significant during observation of non-perceived actions relative to pre-stimulus baseline in which no action was presented. As suggested by this latter finding, the MNS might operate even without conscious awareness of actions. Such function of the MNS might result in behavioral phenomenon as the Chameleon effect in which people tend to implicitly imitate others during social interactions (Chartrand and Bargh, 1999). Taken together, the findings above raise the question of how modulation of action perception level affects activity levels across different regions within the MNS.

In the current study, we addressed this issue by examining whether and how modulation of conscious perception of actions modulates the activation and functional distances within various regions of the MNS. To this end, we manipulated perception level by rendering short hand movement videos invisible to conscious perception, and measured the corresponding fMRI BOLD responses in various regions of the MNS. Our results point to two subnetworks within the MNS with different functional properties—one sensitive and one invariant to the level of action perception.

Materials and methods

Participants

Seventeen healthy, right-handed adults (7 males; mean age 26.27, range 19–35 years) participated in this study. Two subjects were excluded from the analysis due to excessive head movement (>2 mm). Participants were recruited from the general population of students at Tel Aviv University and were compensated for their participation with either course credit or payment. Prior to the experiment, all participants provided written informed consent to participate. The study conformed to the guidelines approved by the Tel Aviv University Ethical committee, and the Sheba Medical Center Helsinki committee. In the resting state analysis, we used an open source resting state dataset downloaded from the NITRC project (Neuroimaging Informatics Tools and Resources; https://www.nitrc.org/frs/?group_id=296). The original resting state dataset included 23 subjects (8 males; range 20–40). For comparison purposes with the size of the main experimental dataset, the first 15 subjects (matched in age and gender) were used.

Stimuli

Participants were scanned under four experimental conditions: masked (M) and non-masked (NM) that were presented in either high or low opacity. In the 'M' conditions, perception level was manipulated by using a modification of the continues flash suppression (CFS) paradigm (Tsuchiya and Koch, 2005) to allow masking of short videos rather than static images. By presenting an otherwise visible stimulus of an action video exclusively to one eye while simultaneously presenting strong dynamic noise to the other eye, the CFS procedure allowed us to mask the action videos from visual awareness. Target and masking videos lasted 2 s and overlapped in space. The CFS display consisted of three possible target action videos of different hand movements and three masking videos of different Mondrian patterns. Target videos were presented either with high opacity or low opacity. We used anaglyph glasses with filters of chromatically opposite Red and Cyan colors for the left and right eyes, respectively, such that the target videos were always presented in the cyan-scale (i.e. to the right eye). The mask was therefore always presented in red-scale (i.e. to the left eye). The target stimuli in the 'NM' condition were identical to the 'M' stimuli, and instead of presenting the Mondrian pattern to the left eye, the Mondrian pattern was replaced by a uniform black screen (Figure 1A).

Task

The experiment comprised of a total of six runs corresponding to three masked (M) and three NM runs presented in alternating order. Each masked run comprised of trials with a CFS display (2 s) and an inter-trial interval (ITI) of 8 s during which subjects had to fixate on a cross (+). In order to probe the subjects' perception level throughout the experiment, on one-third of the 'M' condition trials subjects had to provide information regarding their level of perception. Such trials started with the 2 s presentation of the CFS display followed by a 6-s presentation of fixation point. Then, perception level of the subjects was probed by two means—accuracy and confidence. First, subjects were presented with three representative images of the three actions and an empty box corresponding to no perceived action. The location of images on the screen corresponded with four buttons and subjects were instructed to press the button corresponding to the image representing the action they perceived. The location of the images on the screen, and thus the mapping between buttons and action videos, was randomized across trials in order to avoid motor preparation which has been shown to result in BOLD response in MNS regions (Jeannerod, 1999; Cunnington *et al.*, 2006). Finally, the participants reported their

confidence level, namely to what extent they are confident in their report, on a scale from 1 to 4. A report of '4' corresponded to cases in which subjects perceived a sequence of dynamic movements and were sure which action out of the three was displayed. A report of '1' in confidence level corresponded with cases in which subjects did not perceive a movement at all. In case subjects could perceive the action based on a single frame or a flash of an image, they were asked to report an intermediate level of confidence (2 or 3). The time limit for each report was set to 2 s. The NM runs were identical to the masked runs except that we did not probe the subject's perception since in a pretest preceding the experiment we found perception level in the NM condition to be at ceiling (see Procedure). During each NM run we also introduced 6 action execution trials (18 execution trials in total) in which subjects observed for 6 sec a red cross sign instructing them to press rapidly and repetitively with both left and right fingers until the sign disappeared.

In the masked condition, changes in opacity of target video were coupled with changes in perception. Since the two cannot be distinguished, we also used the two different opacities in the NM condition where perception level is at ceiling. During each functional run (either 'M' or 'NM'), half of the trials were presented with high target opacity (H) and half of the trials were presented with low target opacity (L). Trial types were intermixed in a pseudorandom order. Each condition ('M-H', 'M-L', 'NM-H and 'NM-L') consisted of 81 trials in total (27 trials for each one of the three target movements). The subjects reported their perception level (by means of accuracy and confidence level) in 27 'M-H' trials and 27 'M-L' trials. Thus in each subject, perception was probed from 54 masked trials (Figure 1B).

Procedure

The low-opacity level was adjusted for each participant individually in two behavioral pre-tests in order to control perception level. We set the low opacity level such that the target will be invisible in the masked condition, but entirely visible in the NM condition. These pre-tests were conducted inside the scanner right before the main fMRI experiment. The aim of the first pre-test was to determine the low opacity level in which subjects still perceive the target stimulus in the NM condition but not in the masked condition. We presented the CFS stimuli of different actions in random order and probed the subjects' perception as to which action was displayed. Opacity level of target video was varied using the simple up-down staircase procedure (Leek, 2001). In this procedure opacity level was reduced following trials in which the subject's response was correct and opacity level was increased when his\her response was incorrect. We started at the highest (100%) opacity level. Correct responses were followed by a decrease in opacity at constant steps of 18% until an incorrect response occurred. We than started to increase the opacity level in slightly smaller steps of 14.4%. Every time there was a change in the response from correct to incorrect or vice versa, we reduced the step size by 20% from the last step size. The pre-test ended when the opacity level converged and step size was smaller than half percent. We set the low opacity level in the actual experiment to 50% of the opacity level obtained in this pre-test in order to eliminate perception in the masked low-opacity condition. In the second pre-test, we verified the subjects could still fully perceive the targets in the low opacity level of the NM condition (as determined from the previous step). In this pre-test, each of the three hand movement stimuli was presented in the low opacity without a mask ten times in random order, and subjects were asked to report the action perceived (similar to the first pre-test). The opacity level of each subject, determined from the first pre-test, was kept constant during the entire fMRI experiment across the low-opacity masked and NM conditions.

Data acquisition

Functional imaging was performed on a 3T Siemens Magnetom Prisma scanner with a 64 channel head coil located at the Strauss Computational neuroimaging center, Tel-Aviv University. For each subject, 33 interleaved ascending echo-planar T2*-weighted slices were acquired for each volume, covering the brain from the vertex to the occipital lobe (slice thickness = 3 mm, slice gaps = 0 mm, in-plane resolution = 1.718× 1.718 mm, TR = 2000 ms, TE = 35 ms, flip angle = 90°, field of view = 220×220 mm^2, matrix size = 128×128). Masked (M) runs lasted 13:12 min each (396 time points), and 'NM' runs lasted 11:12 min each (336 time points). For anatomical reference, a whole brain high-resolution T1-weighed scan (voxel size 1×1×1 mm) was acquired for each subject. The NITRC resting state dataset was obtained on a 3T General Electric scanner with an 8 channel head coil recorded by Pekar J.J. and Mosofsky S.H. An echo-planar imaging sequence was used to obtain the functional data (TR = 2500 ms; number of time points per subject = 123).

Data analysis

fMRI data analysis was performed using 'Brain Voyager QX' v. 2.8 software package (Brain Innovation, Maastricht, the Netherlands). Data preprocessing included cubic spline slice-time correction, trilinear/sinc three-dimensional (3D) motion correction, temporal high-pass filtering at 0.006 Hz and spatial smoothing with a 6-mm Gaussian (FWHM). Functional images were co-registered to the anatomical scans and both were transformed into the standardized coordinate system of Talairach (Talairach and Tournoux, 1988). Data analysis was performed using the general linear model (GLM).

ROIs localization and analysis

Regions of interest (ROIs; see Figure 3) were defined at the multi subject level. We used a conjunction of two GLM contrasts: NM observation > rest and action execution trials > rest, to reveal brain regions within the mirror neuron network. The resulting map was corrected for multiple comparisons by controlling the false discovery rate (Benjamini and Hochberg, 1995) and thresholded at $q(FDR) < 0.05$, with a minimum cluster size of 15 voxels. A subsequent single subject GLM was performed for all voxels in each ROI, and the average beta estimate across voxels was computed for each condition. Beta values were calculated for the contrast of each experimental condition *vs* rest. In the GLM design matrix, separate regressors were used for observation conditions ('M-H', 'M-L', 'NM-H', 'NM-L'), the perception reports in the masked runs, and the execution trials in the NM runs. Effects of interest were examined using repeated measures analysis of variance (ANOVA) and planned one tailed paired *t* tests with significance level of $\alpha = 0.05$.

Functional dissimilarity analysis

For each subject, we calculated a functional dissimilarity index between BOLD signals across the different mirror regions

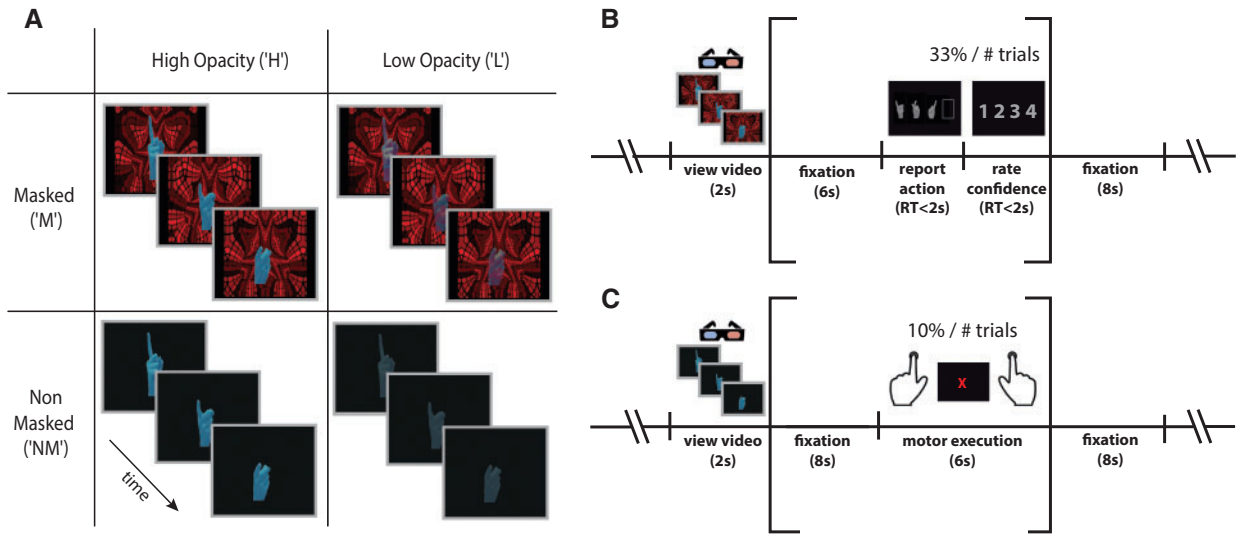

Fig. 1. Experimental design. (A) The experiment included three masked (M) and three non-masked (NM) functional runs presented in alternating fashion. In each run, half of the trials were presented with high target opacity (H) and half of the trials with low target opacity (L) in random order. (B) The 'M' runs comprised of a 2-s CFS display (containing one of three different target videos depicting a specific hand movement presented to one eye, and one of the three masking videos of different Mondrian patterns presented to the other eye). The video was followed by an Inter Trial Interval that lasted 8 s of a fixation cross (+). One-third of the 'M' condition trials were followed by the participants' report of their perception. The participants reported which action was presented and their level of confidence on a scale from 1 to 4. The duration of accuracy and confidence reports was limited to 2 s. The 'NM' runs comprised of a 2 s presentation of the target videos to the right eye and a blank screen to the left eye, followed by an 8 s inter trial interval (ITI) of fixation cross. We also introduced six execution trials at each 'NM' run in which the fixation cross turned red for 6 s, and subjects were instructed to press rapidly and repetitively with both left and right fingers until the fixation cross disappeared.

(see above). This index is based on correlation distance between fMRI time-course in each ROI:

$$d_{i,j} = 1 - \frac{\sum_{k=1}^{n}(x_{i_k} - \bar{x}_i)\cdot\sum_{k=1}^{n}(x_{j_k} - \bar{x}_j)}{\sqrt{\sum_{k=1}^{n}(x_{i_k} - \bar{x}_i)^2}\cdot\sqrt{\sum_{k=1}^{n}(x_{j_k} - \bar{x}_j)^2}}$$

where

$$\bar{x}_i = \frac{1}{n}\cdot\sum_{k=1}^{n} x_{i_k}$$

$$\bar{x}_j = \frac{1}{n}\cdot\sum_{k=1}^{n} x_{jk.}$$

For each defined ROI in each subject, we Z-score normalized the time course of the BOLD signal in each voxel, and averaged the signal across all voxels. This procedure yielded one representative time-course for each ROI. Next, we calculated the distance between the activation of each pair of ROIs using the above dissimilarity measure, yielding a matrix of all pairwise distances. In order to visualize all pair-wise distances between all ROIs, we used classical multi-dimensional scaling (MDS) (Borg and Groenen, 2005). MDS displays the NxN dissimilarity distance matrix between all pairs of regions in a 2D plot such that the distances between ROI pairs are preserved as well as possible. We also examined whether the functional dissimilarity across the different MNS regions remains stable regardless of experimental condition. To this end, we performed the same analysis on resting state data of a separate group of subjects.

Results

Behavioral results

Subjects responded within the time limits to 96.85% of the probe trials (33% of masked trials; see Methods). In two trials on average (6 maximum in one subject) responses were missed. In the NM condition (as measured for low-opacity condition during the second pre-test), subjects reported seeing the target video in 100% of the trials and all trials were also correctly recognized. Since perception in the NM low condition was at ceiling, we did not probe the behavior from NM high opacity trials. In the masked condition (as measured during the main experiment), subjects reported seeing the target video in 97.9 ± 0.8% (mean ± SEM%) of the high-opacity trials, and 22.7 ± 2.3% of the low-opacity trials (Cohen's $d = 10.93$) (Figure 2A). In the high-opacity condition, most of the reported seen trials were also correctly recognized (mean ± SEM%: 81.13 ± 2.9%). In contrast, perception accuracy was markedly reduced in the low-opacity masked condition (32.1 ± 4.6%) (Figure 2B). Accuracy, as reported by the subjects in the low opacity masked condition was not significantly different from chance [33.3%; $t(14) = 0.27$, $P = 0.78$; two-tailed paired t-test]. These accuracy levels corresponded with reported confidence levels. 91.2 ± 2.6% of masked low opacity trials were reported with the lowest confidence level (1) and 93.5 ± 2.2% of the masked high opacity trials were reported with the highest confidence level (4) (Figure 2C). These behavioral results confirm that our experimental manipulation was successful in rendering low opacity actions in the masked condition invisible to perception. Thus while in the NM condition, opacity level did not affect perception (which was at ceiling), in the masked condition opacity level correlated with perception.

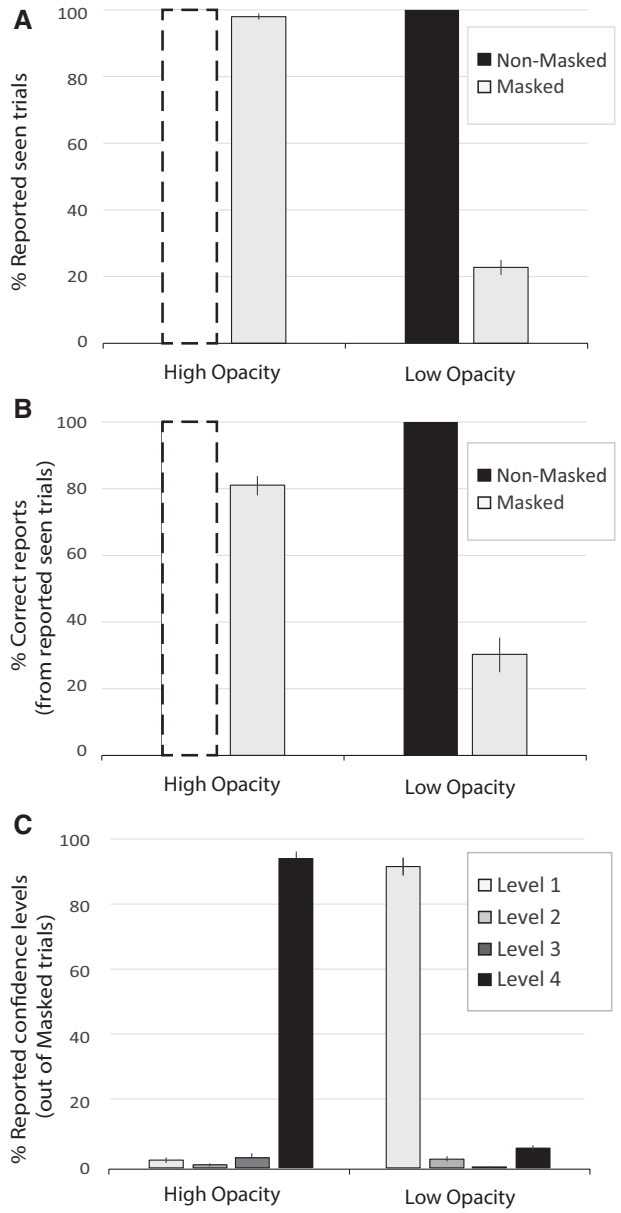

Fig. 2. Behavioral results. (A) Masking in the low-opacity condition resulted in a sharp drop in perception from ceiling (100% in the NM condition) to 22.7% in the masked condition. In the high opacity trials, perception remained high even with masking (97.9%). Since perception was already at ceiling in the NM low-opacity condition, we did not measure it again in the NM high-opacity condition. Dashed bars therefore represent ceiling performance (based on the corresponding low-opacity NM trials). (B) Out of the trials that were reported seen in the masked condition, 81.1% were correctly recognized in high opacity and 32.1% in low opacity. (C) Most trials in the masked high-opacity condition were rated with the highest confidence level, while most trials in the masked low-opacity condition were rated with the lowest confidence level. All bar graphs represent mean group results ($N = 15$) ± SEM across subjects.

ROI localization

We defined ROIs of the putative MNS for all subjects by using a conjunction analysis of observation and execution trials. To this end we performed a GLM conjunction analysis of the contrasts NM observation > rest and execution trials > rest (see Methods for details). We detected 12 regions which included the left primary motor cortex (M1), the left sensory-motor cortex (SMC), the supplementary motor area (SMA), two patches in the right dorsal premotor cortex (PMd), right ventral premotor cortex (PMv), the right inferior frontal gyrus (IFG), right intra parietal sulcus (IPS), the right temporal-parietal junction (TPJ) and posterior superior temporal sulcus, the lateral occipital cortex bilaterally (LOC) and the right primary visual cortex (V1) (see Table 1; Figure 3C). The significant patches of activation in visual areas (V1, LOC), obtained in our localizer are not surprising given that visual stimuli were present both in the observation and execution conditions. Since these visual regions are not considered integral parts of the MNS, we did not include them further in our ROI analysis.

GLM analysis

The time-course of each voxel in the ROIs was fit with a GLM using the standard hemodynamic response function used in BrainVoyager. For each voxel, the beta value for each condition *vs* rest (masked high, masked low, NM high, NM low) was extracted and averaged across all voxels in each ROI. At the group level, we performed a three-way repeated measures ANOVA to the effects of masking (M/NM), opacity level (H/L) and ROI. This analysis revealed main effects for masking [$F(1,14) = 13.78$, $P < 0.01$] and ROI [$F(8,112) = 7.05$, $P < 0.01$]. Interaction effects were reveled for masking and ROI [$F(3,54) = 3.69$, $P < 0.05$], as well as for opacity level and ROI [$F(8,112) = 4.09$, $P < 0.01$]. The three-way interaction was not significant [$F(1,14) = 1.32$, $P = 0.27$]. In our previous EEG study, we found sensitivity to action perception level in frontal electrodes (Simon and Mukamel 2016). Therefore in the current study, we exploited the high anatomical resolution of fMRI to differentiate between various MNS regions based on such sensitivity. To inspect which ROIs were sensitive to differences in the level of action perception, we first examined in which ROIs the masked condition was significantly stronger in the high *vs* low opacity trials (ΔM). These regions include the left M1 [mean difference high − low opacity ± SEM across subjects: 0.35 ± 0.15, $t(14) = 2.22$, $P < 0.05$; one tailed paired *t*-test], the left SMC [0.24 ± 0.09, $t(14) = 2.51$, $P < 0.05$], the right PMd [0.36 ± 0.12, $t(14) = 2.85$, $P < 0.05$] and the right pSTS\TPJ [0.44 ± 0.07, $t(14) = 5.56$, $P < 0.01$]. In order to verify these differences are not attributed to mere changes in opacity level, we compared these differences with the similar subtraction of the low opacity beta value from the high opacity beta in the NM condition (ΔNM). The ROIs in which 'ΔM' was significantly larger than ΔNM included the same ROIs as above: the left M1 [mean difference ΔM − ΔNM ± SEM across subjects: 0.41 ± 0.21; $t(14) = 1.86$, $P < 0.05$], left SMC [0.31 ± 0.08; $t(14) = 3.62$, $P < 0.01$], right PMd [0.34 ± 0.15; $t(14) = 2.19$, $P < 0.05$], and right pSTS\TPJ (0.29 ± 0.11; $t(14) = 2.71$, $P < 0.01$). We considered these ROIs as sensitive to differences in the level of action perception regardless of changes in opacity level. In the remaining ROIs, ΔM (the activation in high relative to low opacity trials in the masked condition), was not significantly different than zero [$t(14) = 0.74$, $P = 0.23$ in the SMA, $t(14) = 0.94$, $P = 0.17$ in right PMv, $t(14) = 1.16$, $P = 0.13$ in the right IFG and $t(14) = 0.71$, $P = 0.24$ in the right SPL]. Additionally, ΔM and ΔNM were not significantly different in the SMA [mean difference ΔM - ΔNM ± SEM across subjects: 0.04 ± 0.05; $t(14) = 0.73$, $P = 0.23$], in the right PMV [0.00 ± 0.22; $t(14) = 0.03$, $P = 0.48$], right IFG [0.03 ± 0.21; $t(14) = 0.15$, $P = 0.43$], and in right SPL [0.10 ± 0.18; $t(14) = 0.55$, $P = 0.29$]. We considered these ROIs as insensitive to differences in the level of action perception (Figure 4). The only regions in which ΔNM was significantly larger than zero was the TPJ

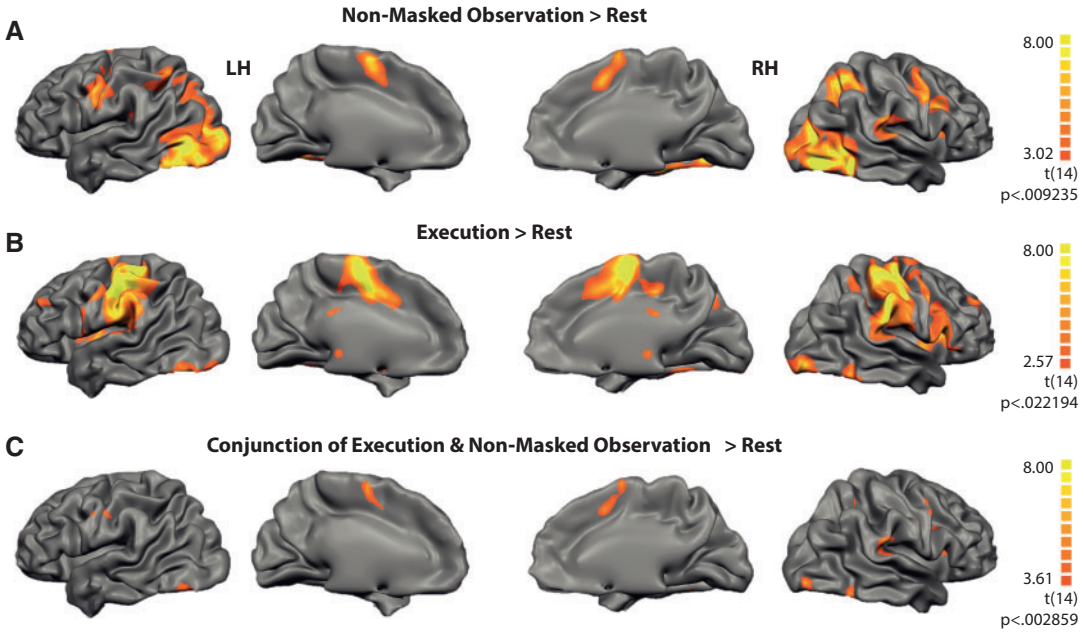

Fig. 3. Localization of the mirror neuron network. Group level (n = 15) RFX GLM maps (corrected for multiple comparisons with q(FDR) < 0.05) using (A) the contrast of NM observation (high and low opacity) *vs* rest, (B) the contrast of Execution *vs* rest and (C) the conjunction of (A) and (B). Regions of interest (ROIs) were defined according to this conjunction.

Table 1. Regions of interest (ROIs) detected by GLM conjunction analysis of the contrasts: execution > rest and non-masked observation > rest trials

Location	Cluster size (no. voxels)	Talairach coordinates (mean activation)		
		x	Y	Z
Left primary motor cortex (M1)	193	−53	−7	40
Left sensorimotor cortex (SMC)	151	−53	−17	40
Supplementary motor area (SMA)	2696	2	1	53
Right dorsal premotor cortex (PMd):				
Superior cluster	255	46	−4	49
Inferior cluster	536	55	−4	43
Right inferior frontal gyrus (IFG)	468	34	17	11
Right ventral premotor cortex (PMv)	415	43	4	30
Right intra-parietal sulcus (IPS)	290	33	−50	46
Right temporal-parietal junction (TPJ) and posterior superior temporal sulcus (pSTS)	2425	57	−35	20
Right lateral occipital cortex (LOC)	1949	38	−57	−16
Left LOC	2345	−37	−64	−16
Right primary visual cortex (V1)	556	31	−87	−7

Note: All regions with cluster size ≥ 15 and FDR corrected ($q < 0.05$) are listed.

[$t(14) = 1.89$, $P < 0.05$]. In all other regions, ΔNM was not significantly different than zero.

Functional dissimilarity analysis

We further examined the relationships within and between the sensitive and insensitive mirror regions with respect to action perception as revealed in the previous step. We performed a functional dissimilarity analysis in which we calculated the functional distances between all ROIs. For each ROI in each subject, we averaged the time-courses of the voxels and concatenated the averaged time-courses across all runs. We then calculated the functional distance between the time-courses of each pair of ROIs. These distances are also visualized in two dimensions using MDS (Figure 5; see Methods for details). The mean functional distance between pairs of sensitive ROIs across subjects was significantly smaller than the mean functional distance between mixed ROI pairs, when one ROI was taken from the sensitive and the other from the insensitive group of regions [mean distance (Md) ± SEM: 0.48 ± 0.01 within sensitive ROIs and 0.69 ± 0.01 between sensitive and insensitive ROIs, $t(14) = 19.43$, $P < 0.001$; two tailed paired *t*-test across subjects]. The same effect was obtained for the insensitive ROIs group [Md ± SEM: 0.47 ± 0.01 within insensitive ROIs, $t(14) = 10.47$, $P < 0.001$]. These results suggest that the MNS ROIs comprise of two sub groups of regions that are functionally distinct with respect to their sensitivity to action perception. There was no significant difference between the mean functional distance

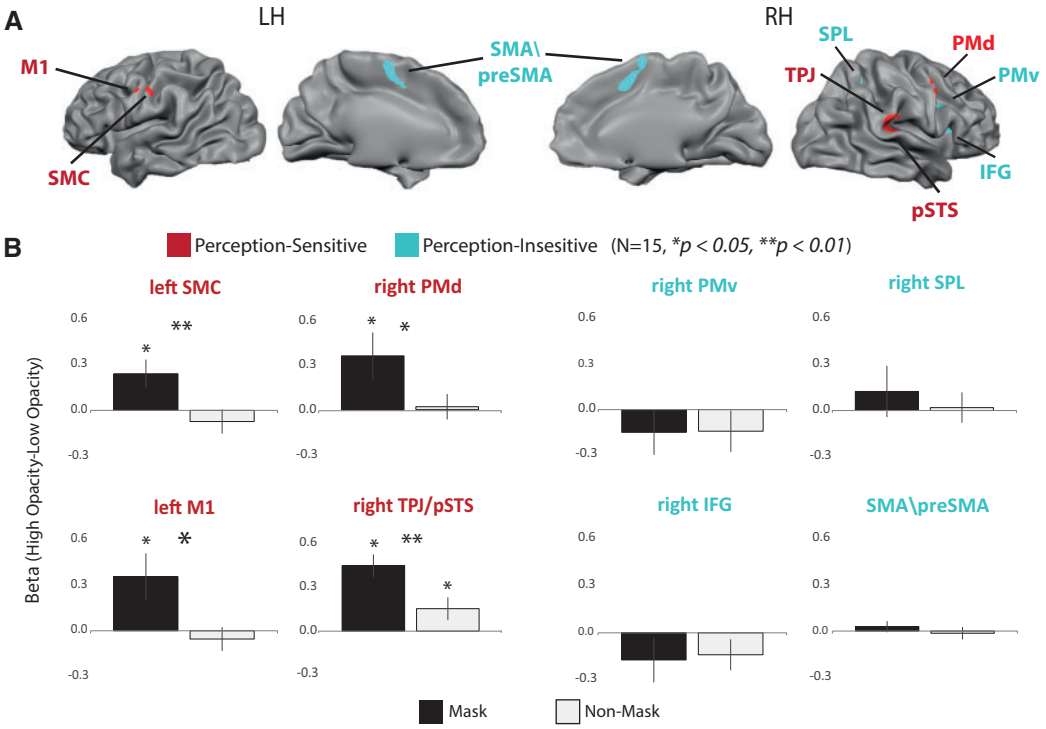

Fig. 4. Differential Sensitivity to Perception level within the mirror neuron network. (A) The conjunction map from Figure 3C, color coded according to sensitive and insensitive regions. Red color coded ROIs were found sensitive to the level of action perception beyond changes in opacity level, whereas the blue color coded ROIs were found insensitive to perception level as defined from the analysis in (B). (B) For each ROI the beta differences between high and low opacities were separately calculated in the masked and NM conditions. In the Masked condition, changes in opacity level corresponded with strong changes in perception level (see figure 2) while in the NM condition perception was not affected. Changes in opacity level resulted in larger beta differences in the masked condition relative to NM condition in the right pMd, right TPJ, left M1 and left SMC. This suggests stronger sensitivity to perception level in these regions (*P < 0.05, **P < 0.01, error bars represent standard error).

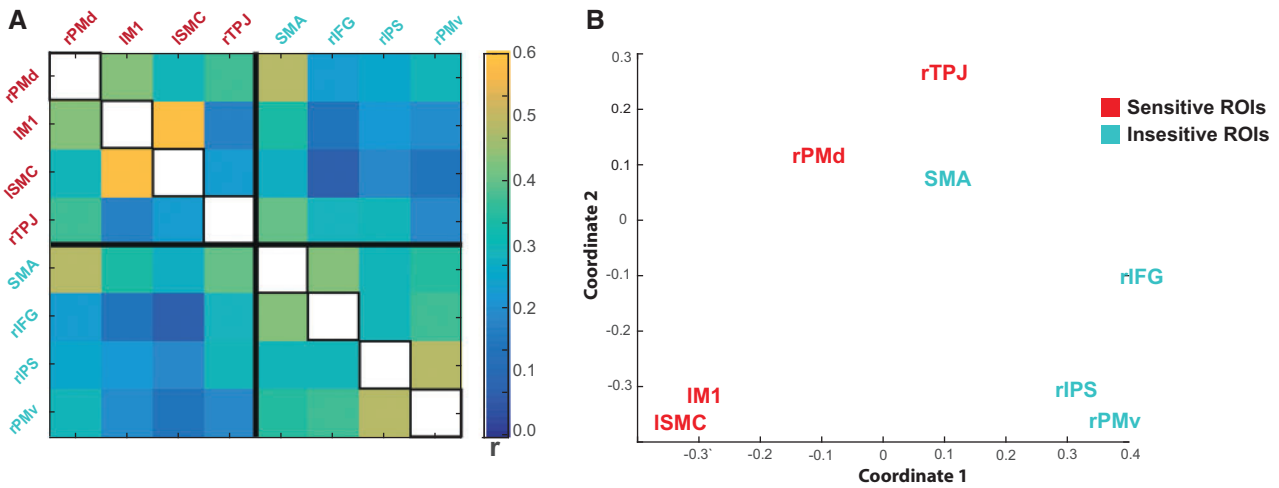

Fig. 5. Functional distances during the experiment time course. (A) Correlation matrix between MNS ROIs based on the concatenated time-courses from all functional runs (see Methods for details). Bold lines delineate the sensitive (red) and insensitive (blue) ROIs as revealed in the GLM analysis. (B) Two-dimensional plot of all functional distances between ROIs using MDS (based on the distance matrix in A). The distances within each group of ROIs (sensitive/insensitive to perception level) are significantly smaller than the distances between the groups (see text).

within the sensitive ROIs relative to the mean functional distances within the insensitive ROIs [$t(14) = 0.49$, $P = 0.63$]. Intrigued by this finding, we were further interested in testing whether this pattern of functional dissimilarity between the mirror ROI subgroups depends on the experimental condition. To that end, we conducted a follow-up exploratory analysis in which we performed the same analysis on resting state data from an additional set of subjects (see methods). Similar to the results obtained with our task data, the mean functional distance during rest between sensitive ROI pairs (Md ± SEM: 0.43 ± 0.03), and the mean distance between insensitive pairs (Md ± SEM: 0.48 ± 0.08), were both smaller relative to the mean distance between mixed pairs [Md ± SEM: 0.61 ± 0.04; $t(14) = 9.07$, $P < 0.001$ for sensitive pairs; $t(14) = 6.13$, $P < 0.001$ for insensitive pairs]. This finding suggests that the partitioning of

MNS ROIs to two distinct subnetworks is more general and holds true beyond their sensitivity to action perception.

Discussion

In the present study, we investigated whether and how perception level modulates the activation magnitude within MNS regions. To this end, we manipulated the perception level of videos depicting different hand movements, and measured corresponding changes in the fMRI BOLD signal. Our results suggest that the MNS can be divided to two functionally distinct sub-networks with respect to their correspondence between activity level and conscious perception of observed actions. Mirror regions that are sensitive to perception level included M1 and SMC in the left hemisphere and PMd, and pSTS/TPJ of the right hemisphere. Mirror regions that were found insensitive to perception level included the SMA, right IFG, PMv and SPL. This parcellation to two subnetworks was also expressed in smaller functional distances between regions within each network relative to regions across the two networks both during task and resting state.

Among the mirror regions we localized in the current study, the sensitive regions (e.g. the left M1, left SMC and the right PMd) seem to share a common function that is tightly linked to action execution mechanisms. The unique presence of most corticospinal projections from the primary motor cortex and PMd of the monkey (Dum and Strick, 1991; He *et al.*, 1993, 1995) suggests that these regions are the only ones within the MNS that may have direct influence on action generation and execution (Stefano, 2015). Many transcranial magnetic stimulation (TMS) studies in humans rely on the motor evoked potentials elicited when stimulating M1 (Priori *et al.*, 1998) and some demonstrate shorter reaction times in response to stimulation of the PMd (Chambers *et al.*, 2007). These evidence add further support to the notion that these regions possibly signal the final output to the muscles necessary for execution of an action. The somatosensory cortex is sensitive to movements of skin and muscles and co-activates with M1 and PMd due to its strong reciprocal connections to them. We recently demonstrated stronger mirror activity, as recorded from electroencephalography (EEG) over the sensorimotor channels, for consciously perceived *vs* non-perceived actions (Simon and Mukamel, 2016). Although the spatial resolution of EEG is low, these channels most probably correspond with activity in the sensorimotor cortices. It is most likely that the effect we found in EEG originates from the sensitive regions as defined in the current study. In the current fMRI study we found that an ROI consisting of the TPJ and extending to the posterior STS is also sensitive to changes in action perception level regardless of opacity level. Several reports have linked the TPJ to spatial (Macaluso and Driver, 2001; Corbetta and Shulman, 2002) and re-orienting (Geng and Vossel, 2013) attentional processes as well as to social interaction (Krall *et al.*, 2015). Converging evidence identified the pSTS as a major hub of the MNS that has a crucial role in action perception and recognition (Grossman *et al.*, 2000; Grossman *et al.*, 2004). Disruption of the function in the pSTS either by transcranial magnetic stimulation (Grossman *et al.*, 2005) or as a result of degenerative brain disease (Nelissen *et al.*, 2010) impairs the perception of biological motion and/or action understanding.

The insensitive regions, in which no activation differences with respect to action perception level were found, are consistently associated with response inhibition mechanisms. Activation during successful response inhibition tasks (e.g. go/no-go, stop signal or Stroop) were reported in the right IFG (Brass *et al.*, 2005; Bien *et al.*, 2009; Chikazoe *et al.*, 2009; Dodds *et al.*, 2011; Sebastian *et al.*, 2013; Erika-Florence *et al.*, 2014; Sebastian *et al.*, 2016), right PMv (Bien *et al.*, 2009; Chikazoe *et al.*, 2009; Dodds *et al.*, 2011; Levy and Wagner, 2011; Sebastian *et al.*, 2013), pre-SMA (Sebastian *et al.*, 2013; Erika-Florence *et al.*, 2014) and parietal regions (Bien *et al.*, 2009; Sebastian *et al.*, 2013). Virtual lesions induced by TMS to the IFG (Chambers *et al.*, 2007; Swann *et al.*, 2012) and pre-SMA (Swann *et al.*, 2012; Obeso *et al.*, 2013) impaired inhibition performance. Enhanced activations in the PMv, SMA, IFG and SPL were found during response inhibition while anticipating a reward (Rosell-Negre *et al.*, 2014), and during expectation for a stop signal to occur (Vink *et al.*, 2015). The mirror system may be utilized for perceptual anticipation and prediction of ongoing actions time courses (Chaminade *et al.*, 2001; Kilner *et al.*, 2007; Lamm *et al.*, 2007; Schubotz, 2007), and evidence for the involvement of the IFG (Hampshire *et al.*, 2010; Avenanti *et al.*, 2013) and PMv (Bischoff *et al.*, 2014) in this process have been reported. The lack of differences in the current study between perceived and not perceived conditions in these regions could be a result of top-down expectation of an impending action to appear in the non-perceived trials of the masked-low condition. We cannot rule out the possibility that greater anticipation in the non-perceived trials might increase the activity in these regions and narrow the differences between perceived and non-perceived trials.

Our parcellation of the MNS to sensitive/insensitive regions with respect to action perception goes along with the earlier reports of differential sensitivity within MNS to action inhibition and anticipation. Our finding that functional distance patterns remained similar across perception task and resting state conditions even in a separate group of subjects, suggest that each group of MNS regions might consist a somewhat independent functional network regardless of task. This idea is further supported by a study of Molinari *et al.* (2013) using independent component analysis on resting-state and action observation task fMRI data. The study identified two networks with good spatial correspondence between task and rest related maps. The first network included portions of the anterior parietal cortex including the somatosensory cortex and dorsal parts of the premotor cortex in proximity to M1 corresponding with our sensitive regions network. The second network included more posterior portions of the parietal lobe and more ventral premotor parts extending toward the IFG corresponding with our insensitive network. The activity of these networks is at least in part supported by direct anatomical connections between their nodes (Molinari *et al.*, 2013). In a meta-analytic connectivity study, modeling of the IFG independent of employed paradigm, determined the strongest functional connections for the right IFG with the left IFG/Insula, bilateral portions of the ventral premotor cortex, SMA and pre-SMA corresponding to the insensitive network (Sebastian *et al.*, 2016). Taken together these data support the existence of two sub networks within the mirror system which as our current study suggests differ also on the dimension of sensitivity to action perception level.

In the current study, we distinguished between two neuroanatomical networks within the MNS with respect to their sensitivity to the level of action perception. To date, the discussion regarding the functional role of the MNS in action and intention understanding has mostly addressed this system as a whole, and possible functional variability between the different nodes has been less emphasized. The current results support the notion that the MNS comprises of (at least) two subsystems. Given that action understanding requires conscious perception, the

current results contribute to the discussion concerning the functional role of the different regions within the MNS to this important cognitive function.

Funding

This study was supported by the I-CORE Program of the Planning and Budgeting Committee and The Israel Science Foundation (grant No. 51/11), The Israel Science Foundation (grants Nos 1771/13 and 2043/13), and Human Frontiers Science Project (HFSP) Career Development Award (CDA00078/2011-C) (R.M.); The Sagol School of Neuroscience fellowship (S.S.). The funders had no role in study design, data collection and analysis, decision to publish, or preparation of the manuscript.

Acknowledgements

The authors thank, O. Ossmy, R. Gilron, D. Reznik, M. Mazor and L. Mudrik for their fruitful comments on the manuscript.

Conflict of interest. None declared.

References

Avenanti, A., Annella, L., Candidi, M., Urgesi, C., Aglioti, S.M. (2013). Compensatory plasticity in the action observation network: virtual lesions of STS enhance anticipatory simulation of seen actions. *Cerebral Cortex*, **23**(3), 570–80.

Benjamini, Y., Hochberg, Y. (1995). Controlling the false discovery rate: a practical and powerful approach to multiple testing. *Journal of the Royal Statistical Society. Series B (Methodological)*, **57**(1), 289–300.

Bien, N., Roebroeck, A., Goebel, R., Sack, A.T. (2009). The Brain's intention to imitate: the neurobiology of intentional versus automatic imitation. *Cerebral Cortex*, **19**(10), 2338–51.

Bischoff, M., Zentgraf, K., Pilgramm, S., Stark, R., Krueger, B., Munzert, J. (2014). Anticipating action effects recruits audiovisual movement representations in the ventral premotor cortex. *Brain and Cognition*, **92**, 39–47.

Borg, I., Groenen, P.J. (2005). *Modern Multidimensional Scaling: Theory and Applications*. Springer Science & Business Media.

Brass, M., Derrfuss, J., von Cramon, D.Y. (2005). The inhibition of imitative and overlearned responses: a functional double dissociation. *Neuropsychologia*, **43**(1), 89–98.

Caspers, S., Zilles, K., Laird, A.R., Eickhoff, S.B. (2010). ALE meta-analysis of action observation and imitation in the human brain. *Neuroimage*, **50**(3), 1148–67.

Catmur, C., Mars, R.B., Rushworth, M.F., Heyes, C. (2011). Making mirrors: premotor cortex stimulation enhances mirror and counter-mirror motor facilitation. *Journal of Cognitive Neuroscience*, **23**(9), 2352–62.

Catmur, C., Walsh, V., Heyes, C. (2007). Sensorimotor learning configures the human mirror system. *Current Biology*, **17**(17), 1527–31.

Chambers, C.D., Bellgrove, M.A., Gould, I.C., *et al.* (2007). Dissociable mechanisms of cognitive control in prefrontal and premotor cortex. *Journal of Neurophysiology*, **98**(6), 3638–47.

Chaminade, T., Meary, D., Orliaguet, J.P., Decety, J. (2001). Is perceptual anticipation a motor simulation? A PET study. *Neuroreport*, **12**(17), 3669–74.

Chartrand, T.L., Bargh, J.A. (1999). The chameleon effect: the perception-behavior link and social interaction. *Journal of Personality and Social Psychology*, **76**(6), 893–910.

Chikazoe, J., Jimura, K., Asari, T., *et al.* (2009). Functional dissociation in right inferior frontal cortex during performance of go/no-go task. *Cerebral Cortex*, **19**(1), 146–52.

Corbetta, M., Shulman, G.L. (2002). Control of goal-directed and stimulus-driven attention in the brain. *Nature Reviews Neuroscience*, **3**(3), 201–15.

Csibra, G. (2007). Action mirroring and action understanding: an alternative account. In Haggard, P., Rossetti, Y., Kawato, M., editors. *Sensorimotor Foundations of Higher Cognition*. Oxford: Oxford University Press.

Cunnington, R., Windischberger, C., Robinson, S., Moser, E. (2006). The selection of intended actions and the observation of others' actions: A time-resolved fMRI study. *Neuroimage*, **29**(4), 1294–302.

Del Giudice, M., Manera, V., Keysers, C. (2009). Programmed to learn? The ontogeny of mirror neurons. *Developmental Science*, **12**(2), 350–63.

Dipellegrino, G., Fadiga, L., Fogassi, L., Gallese, V., Rizzolatti, G. (1992). Understanding motor events - a neurophysiological study. *Experimental Brain Research*, **91**(1), 176–80.

Dodds, C.M., Morein-Zamir, S., Robbins, T.W. (2011). Dissociating inhibition, attention, and response control in the frontoparietal network using functional magnetic resonance imaging. *Cerebral Cortex*, **21**(5), 1155–65.

Dum, R.P., Strick, P.L. (1991). The origin of corticospinal projections from the premotor areas in the frontal-lobe. *Journal of Neuroscience*, **11**(3), 667–89.

Erika-Florence, M., Leech, R., Hampshire, A. (2014). A functional network perspective on response inhibition and attentional control. *Nature Communications*, **5**, doi:10.1038/ncomms5073.

Fogassi, L., Ferrari, P.F., Gesierich, B., Rozzi, S., Chersi, F., Rizzolatti, G. (2005). Parietal lobe: from action organization to intention understanding. *Science*, **308**(5722), 662–7.

Gallese, V., Fadiga, L., Fogassi, L., Rizzolatti, G. (1996). Action recognition in the premotor cortex. *Brain*, **119** (Pt 2), 593–609.

Gallese, V., Fadiga, L., Fogassi, L., Rizzolatti, G. (2002). Action representation and the inferior parietal lobule. In Prinz, W., Hommel, B., editors. *Common Mechanisms in Perception and Action*, Vol. **19**, pp. 334–355.

Gazzola, V., Keysers, C. (2009). The observation and execution of actions share motor and somatosensory voxels in all tested subjects: single-subject analyses of unsmoothed fMRI data. *Cerebral Cortex*, **19**(6), 1239–55.

Geng, J.J., Vossel, S. (2013). Re-evaluating the role of TPJ in attentional control: contextual updating? *Neuroscience and Biobehavioral Reviews*, **37**(10), 2608–20.

Grossman, E., Donnelly, M., Price, R., *et al.* (2000). Brain areas involved in perception of biological motion. *Journal of Cognitive Neuroscience*, **12**(5), 711–20.

Grossman, E.D., Battelli, L., Pascual-Leone, A. (2005). Repetitive TMS over posterior STS disrupts perception of biological motion. *Vision Research*, **45**(22), 2847–53.

Grossman, E.D., Blake, R., Kim, C.Y. (2004). Learning to see biological motion: brain activity parallels behavior. *Journal of Cognitive Neuroscience*, **16**(9), 1669–79.

Hampshire, A., Chamberlain, S.R., Monti, M.M., Duncan, J., Owen, A.M. (2010). The role of the right inferior frontal gyrus: inhibition and attentional control. *Neuroimage*, **50**(3), 1313–9.

He, S.Q., Dum, R.P., Strick, P.L. (1993). Topographic organization of corticospinal projections from the frontal-lobe - motor areas

on the lateral surface of the hemisphere. *Journal of Neuroscience*, **13**(3), 952–80.
He, S.Q., Dum, R.P., Strick, P.L. (1995). Topographic organization of corticospinal projections from the frontal-lobe - motor areas on the medial surface of the hemisphere. *Journal of Neuroscience*, **15**(5), 3284–306.
Heyes, C. (2010). Where do mirror neurons come from? *Neuroscience and Biobehavioral Reviews*, **34**(4), 575–83.
Hickok, G. (2009). Eight problems for the mirror neuron theory of action understanding in monkeys and humans. *Journal of Cognitive Neuroscience*, **21**(7), 1229–43.
Hickok, G. (2013). Do mirror neurons subserve action understanding? *Neuroscience Letters*, **540**, 56–8.
Iacoboni, M., Molnar-Szakacs, I., Gallese, V., Buccino, G., Mazziotta, J.C., Rizzolatti, G. (2005). Grasping the intentions of others with one's own mirror neuron system. *PLoS Biology*, **3**(3), 529–35.
Jeannerod, M. (1999). The 25th Bartlett Lecture. To act or not to act: perspectives on the representation of actions. *The Quarterly Journal of Experimental Psychology. A, Human Experimental Psychology*, **52**(1), 1–29. Available: https://www.scopus.com/inward/record.url?eid=2-s2.0-0033071932&partnerID=40&md5=f9829807882e351ea073f0dc0a1e5f7b. Accessed 10 February 2017
Kilner, J.M., Friston, K.J., Frith, C.D. (2007). The mirror-neuron system: a Baynesian perspective. *Neuroreport*, **18**(6), 619–23.
Krall, S.C., Rottschy, C., Oberwelland, E., *et al.* (2015). The role of the right temporoparietal junction in attention and social interaction as revealed by ALE meta-analysis. *Brain Structure & Function*, **220**(2), 587–604.
Lamm, C., Fischer, M.H., Decety, J. (2007). Predicting the actions of others taps into one's own somatosensory representations - a functional MRI study. *Neuropsychologia*, **45**(11), 2480–91.
Leek, M.R. (2001). Adaptive procedures in psychophysical research. *Perception & Psychophysics*, **63**(8), 1279–92.
Levy, B.J., Wagner, A.D. (2011). Cognitive control and right ventrolateral prefrontal cortex: reflexive reorienting, motor inhibition, and action updating. In Miller, M.B., Kingstone, A. editors. *Year in Cognitive Neuroscience*, Vol. **1224**, pp. 40–62.
Macaluso, E., Driver, J. (2001). Spatial attention and crossmodal interactions between vision and touch. *Neuropsychologia*, **39**(12), 1304–16.
Mele, S., Mattiassi, A.D.A., Urgesi, C. (2014). Unconscious processing of body actions primes subsequent action perception but not motor execution. *Journal of Experimental Psychology-Human Perception and Performance*, **40**(5), 1940–62.
Molenberghs, P., Cunnington, R., Mattingley, J.B. (2012). Brain regions with mirror properties: a meta-analysis of 125 human fMRI studies. *Neuroscience and Biobehavioral Reviews*, **36**(1), 341–9.
Molinari, E., Baraldi, P., Campanella, M., *et al.* (2013). Human parietofrontal networks related to action observation detected at rest. *Cerebral Cortex*, **23**(1), 178–86.
Mukamel, R., Ekstrom, A.D., Kaplan, J., Iacoboni, M., Fried, I. (2010). Single-neuron responses in humans during execution and observation of actions. *Current Biology*, **20**(8), 750–6.
Nelissen, N., Pazzaglia, M., Vandenbulcke, M., *et al.* (2010). Gesture discrimination in primary progressive aphasia: the intersection between gesture and language processing pathways. *Journal of Neuroscience*, **30**(18), 6334–41.
Obeso, I., Cho, S.S., Antonelli, E., *et al.* (2013). Stimulation of the pre-SMA influences cerebral blood flow in frontal areas involved with inhibitory control of action. *Brain Stimulation*, **6**(5), 769–76.
Press, C., Gillmeister, H., Heyes, C. (2007). Sensorimotor experience enhances automatic imitation of robotic action. *Proceedings of the Royal Society B-Biological Sciences*, **274**(1625), 2509–14.
Priori, A., Berardelli, A., Rona, S., Accornero, N., Manfredi, M. (1998). Polarization of the human motor cortex through the scalp. *Neuroreport*, **9**(10), 2257–60.
Rizzolatti, G., Fadiga, L., Gallese, V., Fogassi, L. (1996). Premotor cortex and the recognition of motor actions. *Cognitive Brain Research*, **3**(2), 131–41.
Rizzolatti, G., Fogassi, L. (2014). The mirror mechanism: recent findings and perspectives. *Philosophical Transactions of the Royal Society B-Biological Sciences*, **369**(1644), doi:10.1098/rstb.2013.0420.
Rizzolatti, G., Sinigaglia, C. (2010). The functional role of the parieto-frontal mirror circuit: interpretations and misinterpretations. *Nature Reviews Neuroscience*, **11**(4), 264–74.
Rosell-Negre, P., Bustamante, J.C., Fuentes-Claramonte, P., Costumero, V., Benabarre, S., Barros-Loscertales, A. (2014). Reward anticipation enhances brain activation during response inhibition. *Cognitive, Affective, & Behavioral Neuroscience*, **14**(2), 621–34.
Schubotz, R.I. (2007). Prediction of external events with our motor system: towards a new framework. *Trends in Cognitive Sciences*, **11**(5), 211–8.
Sebastian, A., Jung, P., Neuhoff, J., *et al.* (2016). Dissociable attentional and inhibitory networks of dorsal and ventral areas of the right inferior frontal cortex: a combined task-specific and coordinate-based meta-analytic fMRI study. *Brain Structure & Function*, **221**(3), 1635–51.
Sebastian, A., Pohl, M.F., Kloppel, S., *et al.* (2013). Disentangling common and specific neural subprocesses of response inhibition. *Neuroimage*, **64**, 601–15.
Simon, S., Mukamel, R. (2016). Power modulation of electroencephalogram mu and beta frequency depends on perceived level of observed actions. *Brain and Behavior*, doi:10.1002/brb3.494
Stefano, R. (2015). The neuroanatomy of the mirror neuron system. In Ferrari, P.F., Rizzolatti, G., editors. *New Frontiers in Mirror Neurons Research*, pp. 3–22. New York: Oxford University Press.
Swann, N.C., Cai, W.D., Conner, C.R., *et al.* (2012). Roles for the pre-supplementary motor area and the right inferior frontal gyrus in stopping action: electrophysiological responses and functional and structural connectivity. *Neuroimage*, **59**(3), 2860–70.
Talairach, J. Tournoux, T. (1988). *Co-Planar Stereotaxic Atlas of the Human Brain. 3-Dimensional Proportional System: An Approach to Cerebral Imaging*. New York: Thieme.
Tsuchiya, N., Koch, C. (2005). Continuous flash suppression reduces negative afterimages. *Nature Neuroscience*, **8**(8), 1096–101.
Umilta, M.A., Escola, L., Intskirveli, I., *et al.* (2008). When pliers become fingers in the monkey motor system. *Proceedings of the National Academy of Sciences of the United States of America*, **105**(6), 2209–13.
Umilta, M.A., Kohler, E., Gallese, V., Fogassi, L., Fadiga, L., Keysers, C. (2001). I know what you are doing: a neurophysiological study. *Neuron*, **31**(1), 155–65.
Urgesi, C., Candidi, M., Avenanti, A. (2014). Neuroanatonnical substrates of action perception and understanding: an anatomic likelihood estimation meta-analysis of lesion-symptom mapping studies in brain injured patients. *Frontiers in Human Neuroscience*, **8**, doi:10.3389/fnhum.2014.00344.
Vink, M., Kaldewaij, R., Zandbelt, B.B., Pas, P., du Plessis, S. (2015). The role of stop-signal probability and expectation in proactive inhibition. *European Journal of Neuroscience*, **41**(8), 1086–94.